DE GRUYTER OPEN

Wrinkled graphene: synthesis and characterization of few layer graphene-like nanocarbons from kerosene

A.V. RAMYA, ANU N. MOHAN, B. MANOJ*

Department of Physics, Christ University, Bengaluru-560 029, Karnataka, India

Wrinkled graphene, derived from a facile thermal decomposition and chemical method, was subjected to various analysis techniques and the results have been reported here. Raman studies revealed the presence of highly graphitized amorphous carbon, which was evident by the appearance of five peaks in the deconvoluted first order spectrum. This result was very well corroborated by the XRD analysis. XPS and FT-IR spectra confirmed the incorporation of oxygen functionalities into the carbon backbone. AFM and SEM images of the sample disclosed a cluster of few-layer wrinkled graphene fragments. TEM images displayed a chain of nearly spherical aggregates of graphene, resembling nanohorns. The resistivity and sheet resistance of the sample were found to be low, making the obtained material a promising candidate for various device applications. Hence, kerosene soot proved to be an efficient precursor for facile synthesis of few layer graphene-like nanocarbon.

Keywords: *hydrocarbon; Hummers' method; wrinkled graphene; nanohorns*

1. Introduction

In the current trends in nanoscience and nanotechnology, carbon nanostructures, especially graphene, play a vital role owing to their unique physical and chemical properties and numerous applications. However, the high production cost and tedious synthesis methods present a bottleneck for the researchers. This could be overcome by developing cost-effective and scalable synthesis techniques using effective precursors. Various precursors such as graphite powder, hydrocarbons and bio-based materials have been used for the production of carbon nanostructures employing different synthesis routes such as chemical vapor deposition (CVD), plasma enhanced CVD, sonication, exfoliation, carbon arc discharge, laser irradiation, pyrolysis, thermal carbonization, etc. [1, 2]. In the earlier studies, it was reported that thermal decomposition of hydrocarbon is by far an efficient, dependable and environment friendly method for large scale synthesis of carbon nanostructures [3, 4].

Graphene membranes, in addition to forming sheets with purely hexagonal carbon rings, sometimes also assume a conical shape. The apex of such cones is defined by disclinations, taking the form of fivefold (or smaller) rings. The single-wall carbon nanohorns (SWNH) form one class of such conical structures. These nanohorns can be formed by vapor-phase carbon deposition onto graphite surfaces or pyrolysis of carbon-containing precursors such as hydrocarbons or CO. It was predicted in 1998 that about 2000 nanohorns would assemble to form roughly spherical aggregates of three types: dahlias, buds and seeds [5].

In the current investigation, wrinkled graphene nanostructures resembling carbon nanohorns were synthesized from kerosene: distillate fraction of crude oil, by thermal decomposition followed by modified Hummers' method.

2. Materials and methods

2.1. Preparation of graphene sheets

The precursor used in this study was kerosene soot (KS), obtained by thermal decomposition

---

*E-mail: manoj.b@christuniversity.in

of kerosene in air. 2 g of KS was mixed with 2 g of sodium nitrate and 100 mL of sulphuric acid and stirred continuously for 15 minutes in an ice bath, followed by dropwise addition of 12 g of potassium permanganate. The mixture was then allowed to cool down for 30 minutes. After removing from the ice bath, the solution was stirred continuously for 48 hours by means of a Teflon coated magnetic stirrer. This was followed by the addition of 184 mL of distilled water, 560 mL of warm water along with 40 mL of hydrogen peroxide and the mixture was left undisturbed for 12 hours. The GO particles (KS1) formed were separated from the solution by centrifugation and washed repeatedly with water and acetone followed by sonication for a period of 20 minutes (SKS1). The samples obtained were designated as intercalated samples. The sample (KS) was dispersed in isopropyl alcohol (IPA) and was ultrasonicated in water (SKS) resulting in the exfoliation of graphite flakes into graphene sheets or few layer graphene.

2.2. Chemical and structural characterization

The samples obtained before and after Hummers' treatment and sonication were analyzed using various structural and morphological characterization techniques such as X-ray diffraction (XRD), Raman spectroscopy, Fourier transform infrared (FT-IR) spectroscopy, X-ray photoelectron spectroscopy (XPS), atomic force microscopy (AFM), scanning electron microscopy (SEM), electron dispersive spectroscopy (EDS) and transmission electron microscopy (TEM). X-ray diffractograms of the samples were obtained using a Bruker AXS D8 Advance X-ray diffractometer. Raman measurements were performed at a wavelength of 514.5 nm using Horiba LABAM-HR spectrometer. The FT-IR spectra were obtained using a Shimadzu FT-IR-8400 spectrometer. The compositional analysis of the samples was carried out using X-ray photoelectron spectroscope (XPS-Omicron ESCA probe). The AFM images were obtained using a NanoSurf Easy Scan2 AFM machine. The SEM-EDS and TEM micrographs of the samples were recorded by means of JSM-6360 A

(JEOL) and JEM-2100 (JOEL) systems, respectively.

3. Results and discussion

3.1. XRD analysis

The X-ray diffractogram of KS1 (Fig. 1) shows a characteristic peak of heterogeneous structure, indicating a mixture of graphite oxide and amorphous carbon at 25.09° as a result of oxidation of KS. Broadening of this peak is due to the relatively smaller size of the graphene layers or the short range ordering. The peak at 43.02° indicates the hexagonal lattice structure of the carbon. The (I_{20}/I_{26}) ratio of KS1 is found to be increased to 0.27 compared to that of KS, due to the inclusion of functional groups in the carbon backbone during oxidation. The d_{002}-spacing of KS1 has increased to 3.4204 Å indicating the defects induced in the graphene planes. L_a, L_c, N and n of KS1 have been determined to be 3.0240 nm, 2.9028 nm, 9 and 25, respectively. L_a is considered as a measure to quantify the dislocations, vacancies and number of graphitic atoms [2, 3, 6, 7]. A considerable decrease in the value of L_a of KS1 indicates the improved quality of the graphene oxide (GO) layers formed.
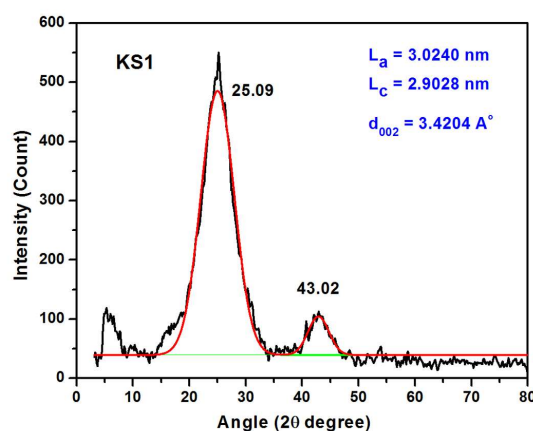

Fig. 1. XRD pattern of KS1.

3.2. AFM analysis

AFM images of KS1 (Fig. 2) show mushroom shaped graphene islands (highlighted in red
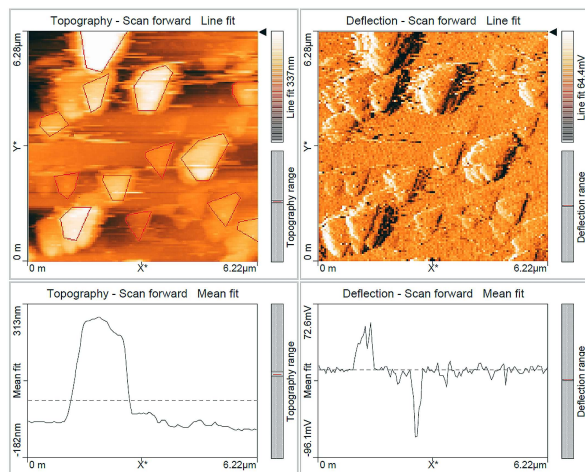
Fig. 2. AFM images of KS1.

Fig. 3. Raman spectrum of KS1.

boundaries), resembling a stratocone. These islands are seen to be stacked one over the other. Height analysis of the KS1 reveals the formation of few-layer wrinkled graphene. These results are very well supported by the XRD analysis.

3.3. Raman analysis

Raman spectrum of KS1 (Fig. 3) exhibits broad and strongly overlapping D (1354 cm^{-1}) and G (1589 cm^{-1}) bands and a broad 2D band (2700 cm^{-1}). An increase in the intensity of the defect band indicates the incorporation of the functional groups. A blue shift of ∼6 cm^{-1} is observed in the case of G band. This can be either due to the presence of D2 band resulting from the defects or the transition of graphite crystal to single graphene sheet [8, 9]. I_D/I_G of KS1 is found to be high (0.91) due to the incorporation of defects during oxidation, thereby disrupting the aromaticity.

Deconvoluted spectrum of KS1 presented in Fig. 4 shows the existence of five peaks, namely, G (∼1589 cm^{-1}), D1 (∼1356 cm^{-1}), D2 (∼1605 cm^{-1}), D3 (∼1487 cm^{-1}) and D4 (∼1210 cm^{-1}). G and D2 bands arise from the graphitic planes whereas D1 band is due to disturbances such as functional groups in the graphene layer. D3 band suggests the amorphous carbon fraction of the soot. D4 can either be due to the sp^2-sp^3 mixed structure or an increase in defects as

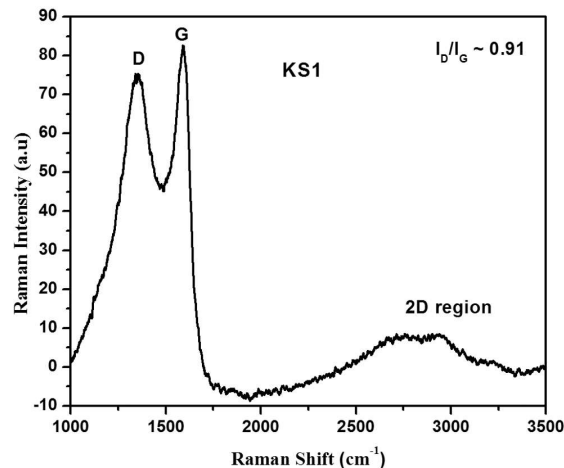a result of oxidation. From Raman analysis, it can be concluded that the oxidative treatment of KS has resulted in the formation of finite sized less defective few-layer GO.
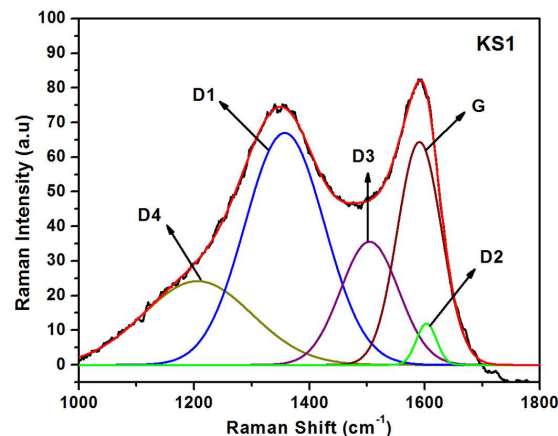

Fig. 4. Deconvoluted first order Raman spectrum of KS1.

3.4. FT-IR analysis

The peak positions in the FT-IR spectrum of KS1 (Fig. 5) clearly indicate the incorporation of hydroxyl (3414 cm^{-1}), epoxy (1044 cm^{-1}, 1168 cm^{-1} and 850 cm^{-1}), carboxyl and carbonyl functional groups into the graphitic lattice of the KS, during oxidation. The peak observed at 1622 cm^{-1} is due to C=C skeletal vibrations
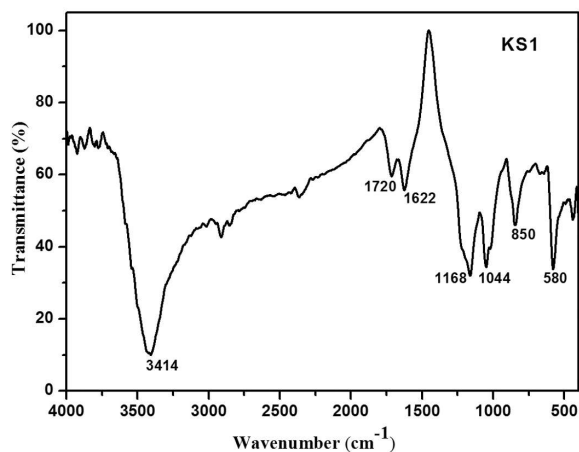
Fig. 5. FT-IR spectrum of KS1.

from graphitic domains and the one at 1720 cm^{-1} is attributed to C=O stretching vibrations of COOH groups situated at the edges and defects of GO lamellae. Yet another peak at 580 cm^{-1} is caused by the C–H out-of-plane bending vibration [10, 11].
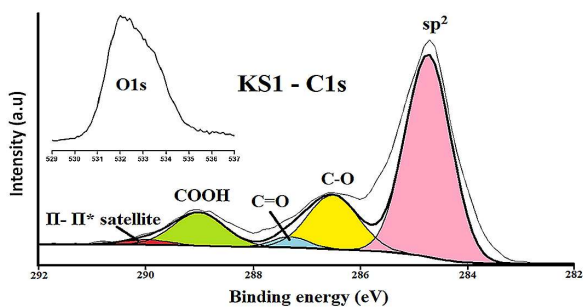

Fig. 6. Deconvoluted C1s XPS spectrum with the inset showing O1s spectrum of KS1.

3.5. XPS analysis

The C1s XPS spectrum of KS1 shown in Fig. 6, clearly indicates four components of carbon atoms in functional groups: the non-oxygenated ring C, i.e. the sp^2 carbon (~284.7 eV), the C in C–O bonds, C bound to O either as epoxy or hydroxyl (~286.5 eV), the carbonyl C, i.e. C=O of alcohols, phenols or ether (~287.3 eV) and the carboxylate carbon, O–C=O (~289.0 eV) [12, 13]. The Π-Π* satellite peak (~290.0 eV) is also observed, which is supported by the UV spectrum [12]. O1s appears

at the binding energy of 532.6 eV as it arises from C=O (531.2 eV), C(=O)–(OH) (531.2 eV) and C–O (533 eV). From the XPS spectrum, the incorporation of functional groups in the KS1 can be deduced, which is also supported by FT-IR results.

3.6. Resistivity measurement studies

Specific resistivity (ρ), sheet resistance and porosity of the prepared graphene nanocarbon, KS and KS1, were obtained by van der Pauw method and the results are presented in Table 1. KS1 showed low value of resistivity (0.168 Ω·cm) and sheet resistance (56.28 Ω/sq) compared to that of KS. Low value of resistivity and decreased sheet resistance of the specific sample makes it an ideal material for the fabrication of devices such as fuel cells or supercapacitors [14, 15].

Table 1. Sheet resistance, resistivity and porosity values of KS and KS1.

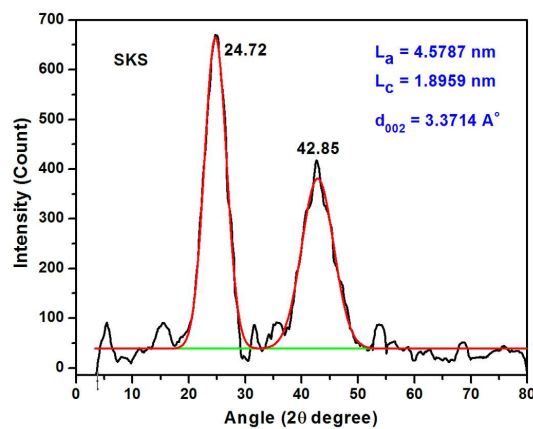| Sample	Sheet Resistance [Ω/sq]	Resistivity [Ω·cm]	Porosity
KS	852.19	2.555	0.048
KS1	56.28	0.168	0.029

Fig. 7. XRD pattern of SKS.

3.7. Investigation on the effect of sonication of carbon nanostructures derived from kerosene

XRD profile of the sonicated kerosene soot (SKS) is presented in Fig. 7. The X-ray
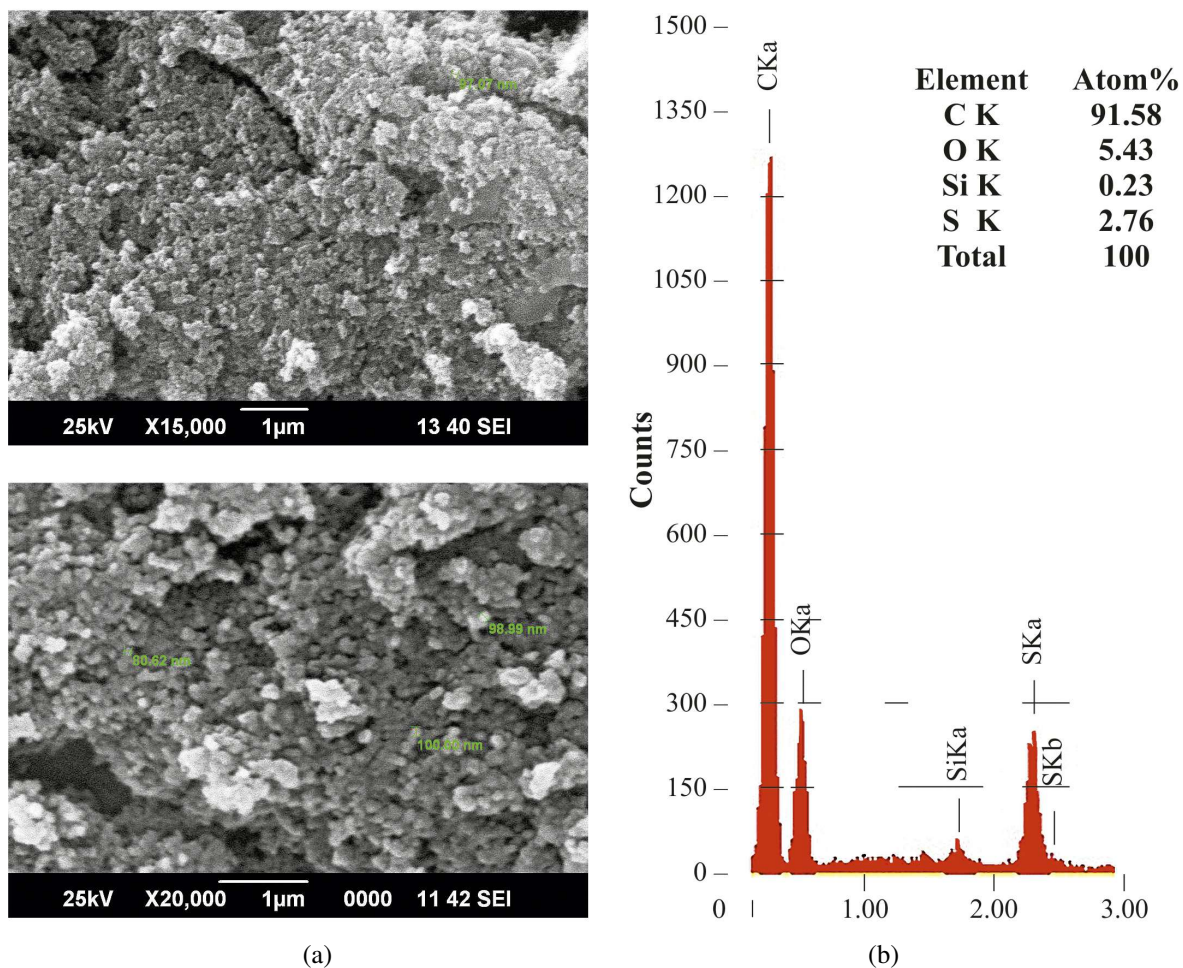
Fig. 8. (a) SEM images of SKS1, (b) EDS spectrum of SKS1.

Element	Atom%
C K	91.58
O K	5.43
Si K	0.23
S K	2.76
Total	100

diffractogram of SKS shows two prominent peaks at $2\theta = 24.72°$ and $42.85°$, respectively. The (0 0 2) peak positioned at $24.72°$ has increased in intensity and shows a lower value of FWHM compared to that of KS, indicating the presence of crystalline graphitic carbon. The broadening of the peak at $42.85°$ upon sonication suggests the presence of amorphous carbon content. The (I_{20}/I_{26}) ratio for the SKS is found to be very low (0.17), thereby confirming the high quality of the carbon nanomaterials. L_a and L_c of the SKS have been determined to be 4.5787 nm and 1.8959 nm, respectively. The d_{002} spacing of the lamellae is 3.3714 Å, which is in a close agreement with that of graphite reported in earlier studies [15–17]. The number of aromatic lamellae (N), average number of carbon atoms per aromatic lamellae (n) and graphitization degree (G) have been calculated to be 6 %, 11 % and 80 %, respectively, which indicates a high order in the stacking of graphene layers.

3.8. SEM analysis

The SEM images of Hummers' treated and sonicated kerosene soot (SKS1) is shown in Fig. 8a. Hummers' treatment has opened up the carbon nanospheres in KS, forming bundles of graphene islands (KS1). Sonication of KS1 resulted in delamination and leaving behind GO fragments. EDS analysis of SKS1 (Fig. 8b) shows that the sample is composed mainly of carbon along with oxygen, silicon and sulfur. The increase in the percentage of oxygen in the sample confirms the oxidation

of KS and incorporation of defects in the carbon backbone.

3.9. TEM analysis

TEM micrographs (Fig. 9) reveal nearly spherical aggregates of graphene fragments, forming interconnected chain-like structures. The magnified TEM image shows that the individual graphene lamellae have rolled up as a result of chemical treatment, to assume a conical shape with a wide apex angle and distorted tubule, resembling nanohorns as reported by Masako et al. in 1999 [5]. Nanohorns are the major subclasses of nanocones, distinguished by an aggregate microstructure. The nanohorn aggregates are robust and cannot be separated into individual components. The distortion in the tubular structure of the shortened, bumpy nanohorns, seen in the TEM image, could be a result of a trade-off between the van der Waals force of interaction between the adjacent nanohorns and the stiffness of the individual horns, which depends on the diameter of the tubule [18].

4. Conclusions

In the current study, the structural and morphological characteristics of carbon nanostructures synthesized from the hydrocarbon (kerosene) were investigated using various techniques. Atmospheric pyrolysis of kerosene results in kerosene soot (KS). Analysis of KS using XRD and Raman spectroscopy revealed that the formed nanostructures possess crystalline structure with few defects. SEM images showed agglomerated spheroid morphology. KS was further subjected to Hummers' treatment, resulting in the incorporation of oxygen functional groups into the graphite layers, which is evident from the increase in defects in the XRD and Raman analyses. Surface morphological characterization showed that the oxidation process resulted in the unfolding of the nanospheroids to form sheet-like graphite oxide. Inclusion of defects in the carbon backbone was confirmed by FT-IR, XPS and EDS analyses. AFM images portrayed mushroom shaped graphene islands. Sonication of KS resulted in an improved stacking of the graphene layers, which is evident from
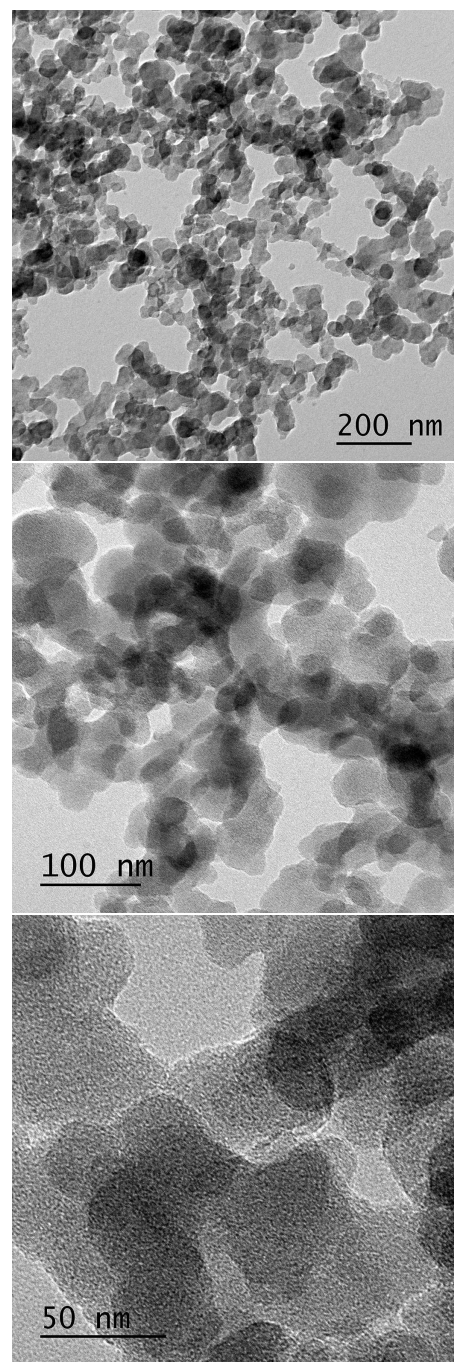

Fig. 9. TEM images of SKS1.

the XRD pattern, however, with an increased amount of amorphous carbon. Resistivity measurements of the sample before and after Hummers' treatment showed a drastic decrease in the resistivity values. The low resistivity values of KS1 indicate that the sample is an ideal candidate

for various device applications. Ultrasonication of KS1 resulted in delamination of graphene oxide sheets, which was confirmed by wrinkled island pattern observed in the SEM images. TEM images suggest the formation of short and bumpy nanohorns, making the sheets an ideal candidate for several potential applications, especially in methane storage, hydrogen-deuterium separation, fuel-cell electrodes, hydrogen generation from methane with steam, capacitors and drug delivery. Thus, in this study, an efficacious synthesis of graphene-like nanocarbon from kerosene for a wide range of applications has been demonstrated.

Acknowledgements

References

[1] SUBRAHMANYAM K.S., VIVEKCHAND S.R.C., GOVINDARAJ A., RAO C.N.R., *J. Mater. Chem.*, 18 (2008), 1517.

[2] MANOJ B., KUNJOMANA A.G., *Russ. J. Appl. Chem.*, 87 (2014), 1726.

[3] COVILLE N.J., MHLANGA S.D., NXUMALO E.N., SHAIKJEE A., *S. Afr. J. Sci.*, 107 (2011), 418.

[4] SADEZKY A., MUCKENHUBER H., GROTHE H., NIESSNER R., PÖSCHL U., *Carbon*, 43 (2005), 173.

[5] MASAKO Y., IIJIMA S., VINCENT H.C., *Single-Wall Carbon Nanohorns and Nanocones*, in: JORIO A., DRESSELHAUS G., DRESSELHAUS M.S. (Eds.), *Carbon Nanotubes*, Springer, Heidelberg, 2008, p. 605.

[6] MOHAN A.N., MANOJ B., *Int. J. Electrochem. Sc.*, 7 (2012), 9537.

[7] VILLEGAS J.P., VALLE J.F.P., RODRIGUEZ J.M.M., GARCIA M.G., *J. Anal. Appl. Pyrol.*, 76 (2006), 103.

[8] MOHAN A.N., MANOJ B., JOHN J., RAMYA A.V., *Asian J. Chem.*, 25 (2013), S76.

[9] KANIYOOR A., RAMAPRABHU S., *AIP Adv.*, 2 (2012), 0321831.

[10] MANOJ B., *Asian J. Chem.*, 26 (2014), 4553.

[11] PIMENTA M.A., DRESSELHAUS G., DRESSELHAUS M.S., CANCADO L.G., JORIO, SAITO R., *Phys. Chem. Chem. Phys.*, 9 (2007), 1276.

[12] CHEN W., YAN L., *Nanoscale*, 2 (2010), 559.

[13] PAREDES J.I., VILLAR R.S., ALONSO A.M., TASCON J.M.D., *Langmuir*, 24 (2008), 10560.

[14] MANOJ B., *Russ. J. Phys. Chem. A*, 89 (2015), 167.

[15] BARO M., VIJAYAN C., RAMAPRABHU S., *J. Nanopart. Res.*, 16 (2014) 7.

[16] MANOJ B., SREELAKSMI S., MOHAN A.N., KUNJOMANA A.G., *Int. J. Electrochem. Sci.*, 7 (2012), 3215.

[17] MANOJ B., RAMYA K., JOHN J., *Int. J. Electrochem. Sci.*, 8 (2013), 9421.

[18] IIJIMA S., YUDASAKA M., YAMADA R., BANDOW S., SUENAGA K., KOKAI F., TAKAHASHI K., *Chem. Phys. Lett.* 309 (1999), 165.